



1 **Lake Surface Temperature Dynamics as Precursors to Glacial Lake**  
2 **Outburst Floods: A Case Study of Lake Merzbacher, Central**  
3 **Tianshan**

4 Meixia Wang<sup>1,2</sup>, Donghui Shangguan<sup>1,2,3\*</sup>, Da Li<sup>1</sup>, Yaojun Li<sup>1</sup>, Rongjun Wang<sup>1</sup>,  
5 Asim Qayyum Butt<sup>1</sup>, Jinkui Wu<sup>1</sup>  
6

7 <sup>1</sup> State Key Laboratory of Cryospheric Science and Frozen Soil Engineering/ Tanggula  
8 Mountain Cryosphere and Environment Observation and Research Station of Tibet  
9 Autonomous Region, Northwest Institute of Eco-Environment and Resources,  
10 Chinese Academy of Sciences, Lanzhou, 730000, China

11 <sup>2</sup> University of Chinese Academy of Sciences, Beijing, 101408, China

12 <sup>3</sup> China-Pakistan Joint Research Centre on Earth Sciences, CAS-HEC, Islamabad,  
13 45320, Pakistan  
14

15 Correspondence: Donghui Shangguan (dhguan@lzb.ac.cn)  
16

17 **Abstract**

18 Glacial lake outburst floods (GLOFs) have become increasingly frequent under climate  
19 warming. Yet the links between lake surface temperature (LST) dynamics and GLOF  
20 triggers remain poorly understood due to the absence of in situ lake temperature  
21 observations. This study investigates the potential of MODIS-derived LST to serve as  
22 a precursor for GLOFs at Lake Merzbacher, a frequently outbursting ice-dammed lake.  
23 We analyzed LST trends from 2000 to 2022 and examined its short-term dynamics  
24 preceding 25 documented GLOF events. Our results reveal a significant summer LST  
25 warming trend of  $0.06 \text{ }^{\circ}\text{C}\cdot\text{yr}^{-1}$ , exceeding the regional air temperature rise. We  
26 identified a critical LST threshold of  $12^{\circ}\text{C}$ , with  $\sim 90\%$  of GLOFs occurring above this  
27 level. More importantly, we detected distinct thermal precursors: a rapid LST increase  
28 (peaking at  $0.65 \text{ }^{\circ}\text{C}\cdot\text{day}^{-1}$ ) beginning  $\sim 8$  days before outburst, and a critical acceleration  
29 phase (exceeding a threshold of  $1.04 \text{ }^{\circ}\text{C}\cdot\text{day}^{-2}$ ) around 9 days pre-GLOF. Furthermore,  
30 the peak discharge of floods showed the strongest correlation with the 15-day  
31 cumulative LST before outburst ( $r = 0.77$ ), highlighting the role of integrated thermal  
32 energy in controlling flood magnitude. This study establishes LST not merely as a  
33 background climate indicator but as a source of diagnostic, short-term warning signals.  
34 We propose a multi-parameter framework integrating absolute LST, its rate of change,



35 and acceleration to enhance early-warning systems for ice-dammed lakes under climate  
36 warming.

37

38 **Keywords:** Lake Merzbacher, GLOF, lake surface temperature, early warning, ice-  
39 dammed lake

40

#### 41 **Copyright statement:**

42 the copyright statement will be included by Copernicus, if applicable.

43

## 44 **1. Introduction**

45 Glacial lake outburst floods (GLOFs) are increasingly recognized as a significant  
46 hazard in High Mountain Asia (HMA), where accelerated atmospheric warming has  
47 driven widespread glacier mass loss and rapid expansion of glacial lakes over recent  
48 decades (Hugonnet et al., 2021; Veh et al., 2023). In the Tianshan Mountains, where  
49 warming rates exceed 0.3°C per decade, glacier retreat has led to the formation and  
50 enlargement of numerous proglacial and ice-dammed lakes, elevating the risk of ice-  
51 dam failure and related floods (Wang et al., 2013; Chen et al., 2016). Ice-dammed lakes  
52 are particularly hazardous because they may drain suddenly and repeatedly, causing  
53 substantial economic damage and loss of life (Carrivick and Tweed, 2016; Shangguan  
54 et al., 2017; Li et al., 2021). Although real-time monitoring systems have improved  
55 early warning capabilities (Zheng et al., 2021), predicting the timing of ice-dam failure  
56 remains difficult due to their complex and often inaccessible settings (Gu et al., 2023).

57 GLOF initiation can result from dynamic external disturbances such as rockfalls,  
58 ice avalanches, or rapid water input, as well as long-term processes that modify dam  
59 stability, including ice melt, permafrost degradation, and evolving subglacial hydrology  
60 (Richardson and Reynolds, 2000; Chikita and Yamada, 2005; Rounce et al., 2016).  
61 Among these drivers, air temperature has been widely linked to GLOFs through its  
62 control on glacier meltwater supply and internal ice-dam weakening (Ng et al., 2007;  
63 Ng and Liu, 2009). Yet, despite its acknowledged importance, the temperature  
64 sensitivity of ice-dammed lakes—and especially the direct response of lake surface  
65 temperature (LST)—remains poorly quantified. Existing models of GLOFs largely  
66 focus on simulating hydrographs (Kingslake and Ng, 2013), with fewer efforts  
67 addressing the environmental conditions that govern outburst timing.

68 Lake Merzbacher, located between the Northern and Southern Inylchek glaciers,



69 represents one of the world's most frequently draining ice-dammed lakes, with  
70 documented GLOFs since 1931 (Mayr et al., 2014). Annual outbursts typically occur  
71 between June and October, coinciding with peak meltwater supply during warm  
72 summer conditions (Ng and Liu, 2009). Previous studies have developed remote-  
73 sensing-based indices to identify pre-outburst signals (Xie et al., 2013) and have  
74 quantified the predictability of the timing of dam failure (Kingslake and Ng, 2013).  
75 However, a key knowledge gap remains: the role of LST dynamics prior to GLOFs has  
76 not yet been systematically evaluated, despite LST being an important indicator of  
77 regional climate forcing and subaqueous ice melt (Austin and Colman, 2007; Zhang et  
78 al., 2014; Debnath et al., 2018; Attiah et al., 2023).

79 In this paper, we investigate whether fluctuations in lake surface temperature can  
80 provide diagnostic information about the timing and magnitude of GLOFs at Lake  
81 Merzbacher. Using MODIS-derived daily LST, we aim to:

- 82 (1) Characterize LST evolution in the days to weeks preceding GLOFs;
- 83 (2) Quantify LST change rates and accelerations as potential early-warning  
84 indicators;
- 85 (3) Evaluate the influence of short-term accumulated temperature on peak flood  
86 discharge.

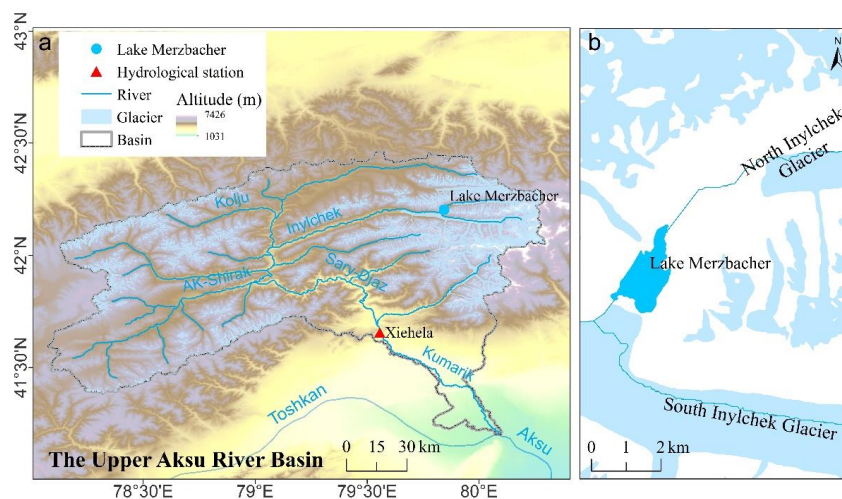
87 These analyses provide new insights into the thermal precursors of ice-dam failure  
88 and contribute to the development of temperature-based monitoring tools for GLOF  
89 hazard assessment in remote alpine environments.

## 90 **2. Study area**

91 Lake Merzbacher is situated in the remote Inylchek region in the central Tianshan  
92 mountain range in Kyrgyzstan, bordering China, at the confluence of the Northern and  
93 Southern Inylchek Glaciers at an altitude of about 3100m, as illustrated in Figure 1. As  
94 described below, Northern Inylchek Glacier terminates in a proglacial lake, and down  
95 valley lies an ice-dammed lake (impounded by Southern Inylchek Glacier) that has  
96 repeatedly outburst to deliver glacier outburst floods (Häusler et al., 2016). Northern  
97 Inylchek Glacier and its neighbour Southern Inylchek Glacier comprise the largest  
98 compound glacier system in the central Tianshan Mountains. Although located in  
99 Kyrgyzstan, both glaciers drain into the Inylchek River. It feeds the Sary-Dshaz River  
100 in Kyrgyzstan, whose runoff flows into the Kumarik River of the main tributary of the  
101 Aksu River in China to feed that country's largest inland river, the Tarim, which  
102 provides a vital water supply to oases around the Taklamakan Desert (Mayr et al., 2014)



103 (Fig. 1a). Glacial meltwater contributes at least 35% of the Tarim's total runoff (Aizen  
104 and Aizen., 1998). This proportion is predicted to rise over the next few decades (Aizen  
105 et al., 2007).



106

107 Figure 1. Map of Lake Merzbacher, in the central Tianshan Mountains.

### 108 3. Data and Methods

#### 109 3.1 Glacial Lake Area and GLOF Records

110 The area of glacial lakes is a key predictor of susceptibility and hazard (Allen et  
111 al., 2019). For Lake Merzbacher, historical lake area from 1990 to 2015 and  
112 documented outburst dates from 2000 to 2015 were obtained from published sources  
113 (Liu, 1993; Glazirin, 2010; Kingslake and Ng, 2013; Shangguan et al., 2017; Li et al.,  
114 2020). Lake area and outburst dates from 2016 to 2022 were extracted from high-  
115 resolution Planet Scope (DOVA) satellite imagery (Table S1, Supplementary Material).  
116 Planet's Dove satellites are CubeSats that weigh 4 kilograms (1000 times lower than  
117 other commercial imaging satellites), 10 by 10 by 30 centimetres in length, width and  
118 height, orbit at a height of about 400 kilometres and provide imagery with a resolution  
119 of 3-5 metres and are envisaged for environmental, humanitarian, and business  
120 applications.

121 For each documented GLOF, the pre-outburst lake area was obtained from the  
122 available satellite imagery. A total of 25 GLOF events from 2000 to 2024 were included  
123 in this study. Since 2000, no GLOF events triggered by glacier surges were reported in  
124 Lake Merzbacher (Liu et al., 2023).



## 125 3.2 Lake Surface Temperature Data

126 Lake surface temperature (LST) was derived from the MODIS Terra Land Surface  
127 Temperature Daily L3 Global 1 km product (MOD11A1). MODIS LST has been shown  
128 to accurately reflect in situ lake temperature measurements at Lake Merzbacher, with  
129  $R^2 = 0.79$  for 2009–2010 observations (Bormudoi et al., 2012).

130 To address missing data, gap-filling was performed using the Climate Forecast  
131 System Version 2 (CFSv2)–MODIS integration in Google Earth Engine, generating  
132 continuous 1 km LST time series (Shiff et al., 2021). The filled dataset (CFSv2\_LST)  
133 was evaluated against the original MODIS LST using mean absolute error (MAE), bias,  
134 and  $R^2$ , yielding high consistency ( $R^2 = 0.95$ , MAE = 1.31°C; Figure S1).

## 135 3.3 LST Temporal Analysis

136 In meteorology, a moving average is commonly used with time series data to  
137 smooth out short-term fluctuations and highlight longer-term trends for mean daily air  
138 temperatures (Hewitson and Crane, 1996). For the filled daily lake surface temperature  
139 (LST) series, the five-day moving average was used to produce smooth LST curves.  
140 Xie et al., (2013) divided Lake Merzbacher into four periods according to the outburst  
141 index: icefall, quick water storage, early-warning and post-drainage. During these four  
142 periods, the lake is filled with water and the water movement is slow; it takes about  
143 one month for an outburst to occur and about a week for the lake to empty after the  
144 drainage (Xie et al., 2013). Therefore, in this paper, the first and second derivative of  
145 the daily LST were calculated for one month before and one week after the glacial lake  
146 outburst.

147 Step 1: Calculate the first derivative of the daily LST to characterize the change  
148 rate of LST ( $^{\circ}\text{C}\cdot\text{day}^{-1}$ ), and analyse the trend of LST before and after the outburst of the  
149 glacial lake.

150 Step 2: Calculate the second derivative of the daily LST to characterize the change  
151 in the rate of temperature change (i.e., acceleration, unit:  $^{\circ}\text{C}\cdot\text{day}^{-2}$ ). A positive value  
152 indicates an accelerating rate of temperature change, while a negative value indicates a  
153 decelerating rate of temperature change.

154 Step 3: Identify the accelerated temperature rise range and calculate the average  
155 value ( $\mu$ ) and standard deviation ( $\sigma$ ) of all the second derivative values during the study  
156 period. Set the threshold for identifying significantly accelerated temperature rise:

157 
$$\text{Threshold} = \mu + 1.5 * \sigma.$$

158 The time regions that satisfy the second derivative of the daily LST > the threshold



159 are defined as periods with significantly accelerated temperature rise.

160 Step 4: For each historical glacial lake outburst event, count the frequency of  
161 significantly accelerated warming areas (i.e., the second derivative of the daily LST >  
162 threshold) within a specific period before its occurrence (the previous 30 days).

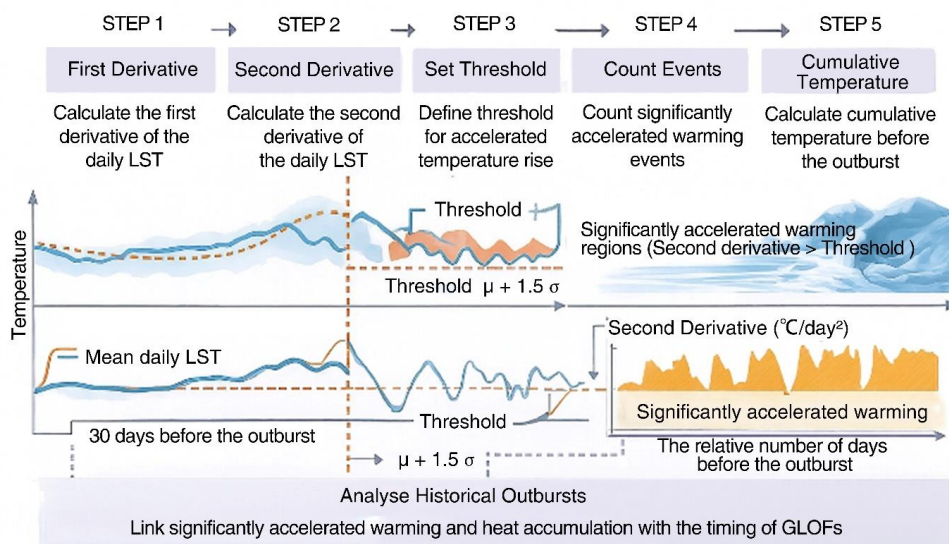
163 Step 5: Calculate the cumulative lake surface temperature in the month before each  
164 glacial lake outburst event (i.e., the sum of the average daily LST during that period).  
165 Cumulative temperature plays a crucial role in the thermodynamic state of glacial lakes  
166 prior to outburst (Liu et al., 2014). By combining with the frequency of significantly  
167 accelerated warming events before the outburst and the cumulative temperature of the  
168 previous month, as recorded in Step 4, this paper will explore the potential association  
169 and influence between these two types of thermal conditions (short-term intense  
170 accelerated warming and longer-term heat accumulation) and the occurrence of GLOFs  
171 (Fig. 2).

172 In the case of a glacial lake, the ice point or pressure-melting point is crucial, which  
173 determines ice ablation and accumulation (Cogley et al., 2011). Lake surface  
174 temperatures above 0°C are considered the effective ablation threshold. The cumulative  
175 lake surface temperature, calculated over consecutive days until the outburst event, is  
176 defined as follows:

$$177 \quad T_A^{(N)} = \sum_{k=1}^N T_k, (k = 1, 2, \dots, N - 1)$$

178 Where  $N$  represents the number of continuous ablation temperature days. The  
179 cumulative temperatures ( $T_A^{(N)}$ ) represents both the cumulative surface temperature of  
180 the lake reaching ablation temperature and the sum of the heat over the period for  $N$   
181 days before the glacial lake outburst.  $T_k$  is the corrected daily average lake surface  
182 temperature. The cumulative temperature change rate is defined as the ratio of the  
183 cumulative temperature difference to the time difference.

184 In this study, to characterize trends in regional terrestrial air temperature, 2 m air  
185 temperatures (T) were obtained from the European Centre for Medium-Range Weather  
186 Forecasts (ECMWF) for the land component of the fifth-generation European  
187 Reanalysis dataset (ERA5-Land) for the period 2000–2022 (Muñoz-Sabater et al.,  
188 2021). Reanalysis data provide a consistent and globally complete description of past  
189 climate, allowing evaluation of regional warming trends relevant to LST dynamics and  
190 GLOF occurrence.



191

192

Figure 2. Thermal conditional and glacial lake outburst floods.

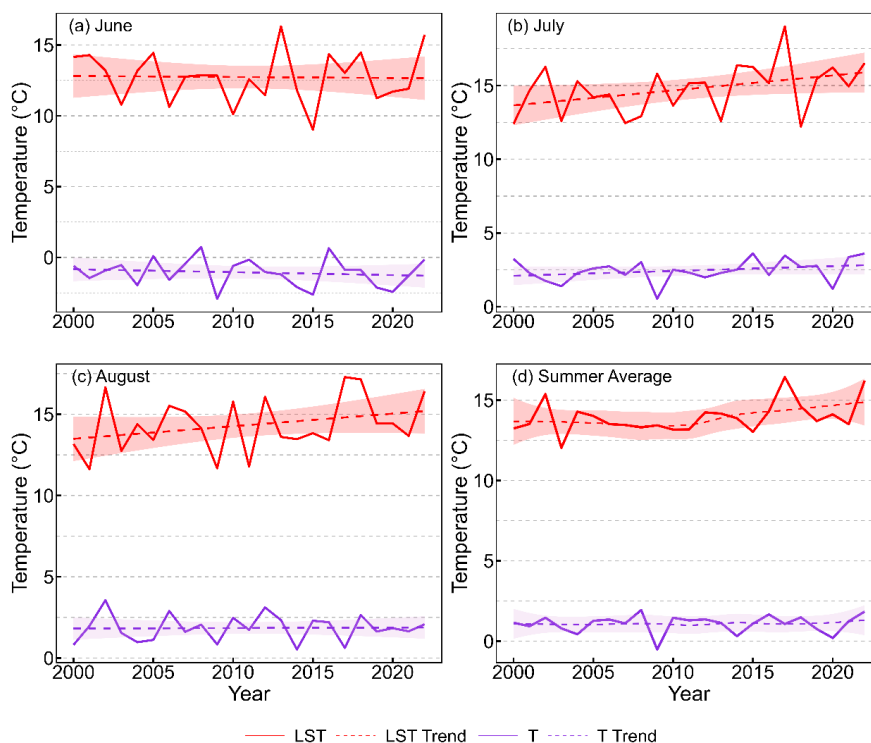
193 **4. Results**

194 **4.1 Temporal Trends of Lake Surface Temperature and Glacial Lake**

195 **Outburst Timing**

196 Between 2000 and 2022, lake surface temperatures (LST) in June, July, August,  
 197 and the summer mean (June–August) exhibited clear upward trends (Fig. 3). Linear  
 198 regression analysis indicates warming rates of approximately  $0.06\text{ }^{\circ}\text{C}\cdot\text{yr}^{-1}$  for the  
 199 summer mean, with July showing the most pronounced increase at  $0.10\text{ }^{\circ}\text{C}\cdot\text{yr}^{-1}$ —twice  
 200 the rates observed in June and August. Mann–Kendall tests confirm that these trends  
 201 are statistically significant ( $p < 0.05$ ) for most LST series. In contrast, air temperature  
 202 (T) exhibits only modest increases with smaller slopes and weaker significance,  
 203 suggesting a stronger warming response at the lake surface than in near-surface air.

204 Satellite image analysis from 1990 to 2024 revealed a declining trend in the glacial  
 205 lake area (Fig. S2a). The average lake area over this period was  $3.22\text{ km}^2$ , with a  
 206 maximum of  $3.95\text{ km}^2$  (9 August 1996) and a minimum of  $2.12\text{ km}^2$  (4 July 2021). The  
 207 timing of glacial lake outburst floods (GLOFs) advanced by approximately 0.6 days per  
 208 year (Fig. S2b), with most post-2000 events occurring from early July to mid-to-early  
 209 August. This shift is attributed to accelerated summer glacier melt and the reduced  
 210 water storage period, highlighting the importance of early-warning and flood mitigation  
 211 strategies.

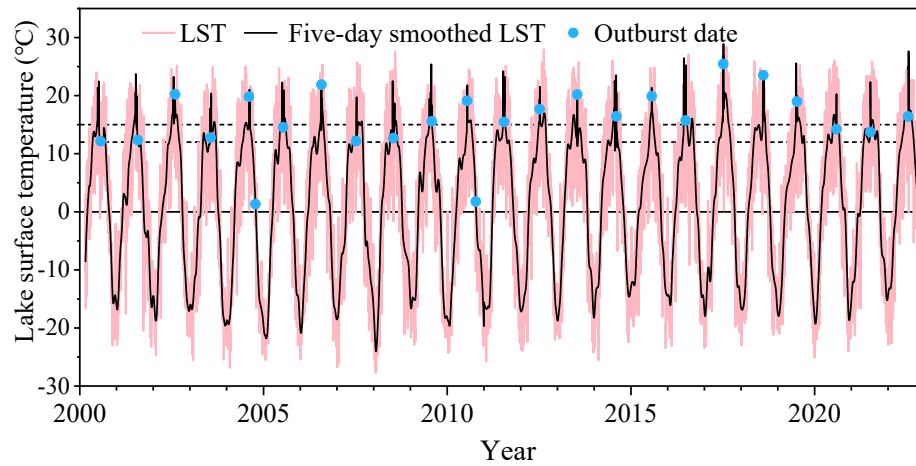


212

213 Figure 3. Time series of lake surface temperature (LST, red line) and air temperature (T,  
214 purple line) for June, July, August, and the mean summer LST (June–August) between  
215 2000 and 2022. Solid lines show annual observations; dashed lines show linear trends  
216 with 95% confidence intervals (shaded).

#### 217 4.2 Short-Term LST Dynamics Before the Glacial Lake Outburst

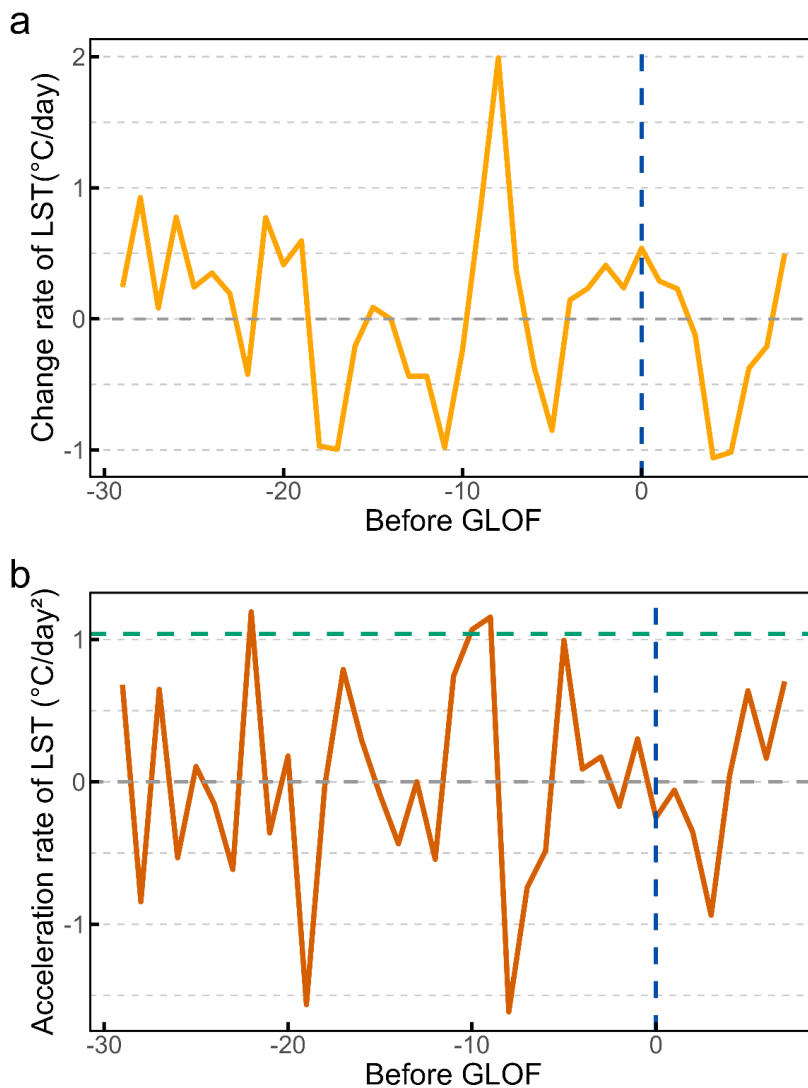
218 Analysis of LST in the 30-day window preceding each GLOF event reveals  
219 characteristic warming patterns (Figs. 4–5). GLOFs predominantly occur on days when  
220 LST exceeds 12 °C, with ~90% of events falling in the 12–20 °C range, suggesting a  
221 critical temperature threshold for ice dam failure. A few extreme events occurred at  
222 LST > 20 °C (e.g., 25.4 °C on 8 July 2017, 23.5 °C on 10 August 2018), likely associated  
223 with heatwaves and intensified ablation (Chikita et al., 2000).



224

225 Figure 4. Lake surface temperature fluctuations in Lake Merzbacher from 2000 to 2022.

226 Blue dot represents the outburst date of the glacial lake.



227

228 Figure 5. LST characteristics before and after GLOFs. (a) Rate of LST change ( $dLST/dt$ )  
229 highlighting pre-outburst warming. (b) Acceleration change rate of Pre-outburst LST  
230 evolution. Blue dashed line represents the outburst date of the glacial lake. Horizontal  
231 green dashed lines indicate critical thresholds:  $1.04\text{ }^{\circ}\text{C}\cdot\text{day}^{-2}$ .

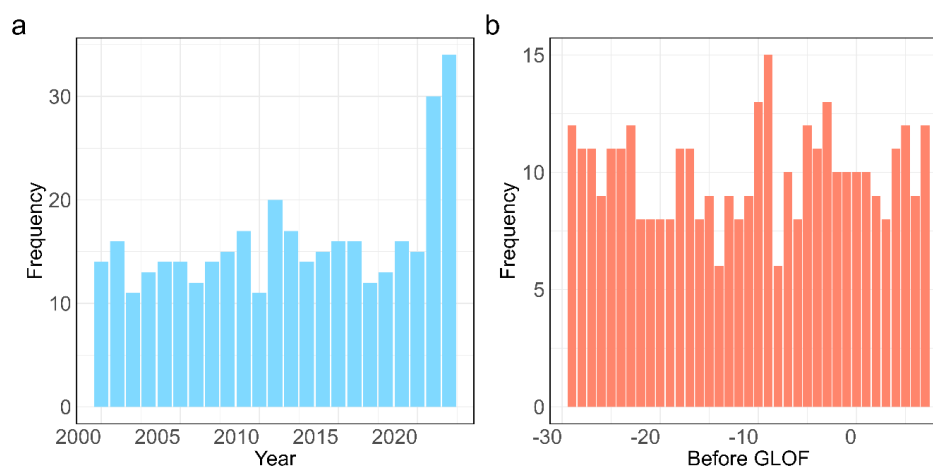
232 Statistical analysis shows a rapid LST increase within approximately eight days  
233 before outbursts (Fig. 5a). A two-sample t-test confirms the presence of a short-term  
234 warming signal prior to GLOFs ( $p < 0.05$ ). On the outburst day, the rate of LST change



235 peaks at  $0.65\text{ }^{\circ}\text{C}\cdot\text{day}^{-1}$ .

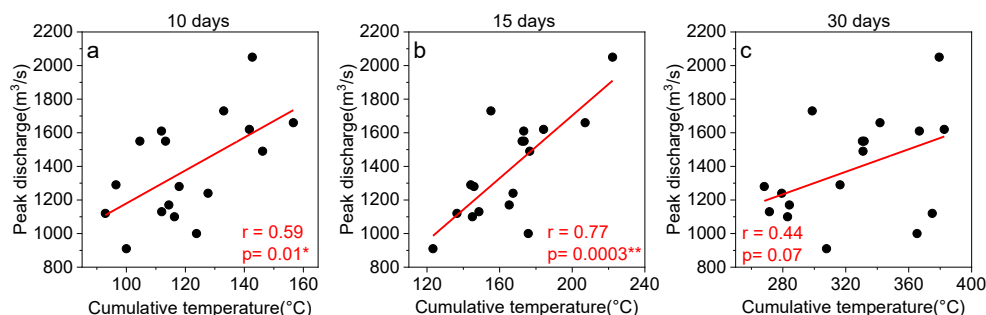
236 To quantify thermal acceleration, the second derivative of LST was computed over  
 237 a 30-day window centered on each outburst. Based on 25 historical events (Table S1),  
 238 a critical acceleration threshold of  $1.04\text{ }^{\circ}\text{C}\cdot\text{day}^{-2}$  was identified. Two exceedances were  
 239 observed: 22 days before the outburst ( $1.20\text{ }^{\circ}\text{C}\cdot\text{day}^{-2}$ ) and 9 days before the outburst  
 240 ( $1.16\text{ }^{\circ}\text{C}\cdot\text{day}^{-2}$ ). The earlier signal may indicate the onset of accelerated thermal activity,  
 241 while the latter corresponds to a pre-outburst thermal reinforcement phase, potentially  
 242 defining a critical short-term pre-outburst window for early warning. Post-outburst,  
 243 LST change rates decline rapidly and occasionally turn negative, reflecting system re-  
 244 equilibration and meltwater inflow (Fig. 5b).

#### 245 4.3 Short-Term Cumulative Temperature and Peak Discharge



246  
 247 Figure 6. Accelerated warming events: interannual and pre-outburst temporal patterns.  
 248 annual frequency of accelerated warming events from 2000 to 2022 (a). Temporal  
 249 distribution of accelerated warming events before the outburst (b).

250 The frequency of accelerated warming events has increased in recent years,  
 251 particularly over the past decade, peaking in 2023 (Fig. 6a). From 2000 to the mid-  
 252 2010s, events were distributed relatively uniformly. Temporal analysis relative to  
 253 outburst dates reveals clustering approximately 10 days before GLOFs (Fig. 6b),  
 254 suggesting a thermally driven triggering mechanism. Although acceleration events are  
 255 observed throughout the 30-day pre-outburst window, the localized peak indicates that  
 256 abrupt LST acceleration could serve as a short-term early-warning signal.



257

258 Figure 7. Relationships between short-term cumulative temperature and GLOF peak  
259 peak discharge. Correlation coefficients (r) and significance levels (p) are indicated for 10-,  
260 15-, and 30-day accumulation windows.

261 To investigate the thermal conditions preceding GLOFs, the correlations between  
262 peak discharge and cumulative temperature over 10-day, 15-day, and 30-day windows  
263 before each outburst event were analyzed (Fig. 7). A clear positive relationship was  
264 identified between cumulative temperature and peak discharge for the shorter  
265 accumulation periods. For the 10-day accumulation window, peak discharge increased  
266 significantly with higher cumulative temperature ( $r = 0.59$ ,  $p = 0.01$ ), indicating that  
267 short-term warming strongly influences flood magnitude. The relationship further  
268 strengthened when the accumulation period was extended to 15 days, showing the  
269 highest correlation among the three windows ( $r = 0.77$ ,  $p = 0.0003$ ), suggesting that  
270 thermal forcing integrated over two weeks is an especially strong predictor of flood  
271 magnitude. In contrast, the positive correlation observed for the 30-day accumulation  
272 window was weaker and statistically insignificant ( $r = 0.44$ ,  $p = 0.07$ ). This suggests  
273 that temperatures averaged over longer periods may dilute the short-term thermal signal  
274 most relevant to triggering rapid lake drainage. Overall, these results imply that GLOF  
275 peak discharge is most sensitive to short-term (10–15 day) cumulative warming,  
276 highlighting the importance of rapid pre-event thermal inputs in controlling flood  
277 magnitude.

## 278 5. Discussion

### 279 5.1 Lake Surface Temperature as a Primary Driver of GLOFs

280 This study provides a systematic analysis linking Lake Surface Temperature (LST)  
281 dynamics to Glacial Lake Outburst Floods (GLOFs) at Lake Merzbacher. Our results  
282 demonstrate that the summer LST warming trend ( $0.06^{\circ}\text{C}\cdot\text{yr}^{-1}$  from 2000 to 2022)



283 exceeded the regional air temperature increase. This amplified warming aligns with  
284 observations from other global lakes, such as Lake Superior and lakes on the Tibetan  
285 Plateau, and is likely driven by positive ice-albedo feedback and the high heat capacity  
286 of water, which allows lakes to store more energy than the surrounding atmosphere  
287 (Austin and Colman, 2007; Zhang et al., 2014).

288 Critically, we identified 12°C as a key thermal threshold for GLOFs, with ~90%  
289 of events occurring when LST exceeded this value. This strongly implicates thermal  
290 forcing as a central mechanism in ice-dam failure. Elevated LST likely promotes dam  
291 instability through two primary pathways: (1) by enhancing thermal erosion at the ice-  
292 water contact, directly weakening the dam structure (Thorarinsson, 1939), and (2) by  
293 accelerating overall glacier melt, which raises lake level and increases hydrostatic  
294 pressure, potentially leading to flotation of the ice dam or the rapid expansion of  
295 subglacial conduits (Shen et al., 2009; Ng et al., 2007). The occurrence of GLOFs  
296 during extreme heatwaves (e.g., LST > 20°C in 2017 and 2018) further underscores the  
297 potency of thermal drivers.

## 298 5.2 Pre-Outburst Thermal Dynamics and Early-Warning Potential

299 A significant advancement of this research is the identification of quantifiable  
300 thermal precursors.

301 Short-term warming pulse: the consistent and rapid increase in LST (peaking at  
302 0.65 °C·day<sup>-1</sup>) beginning approximately eight days before an outburst provides a clear  
303 short-term warning signal.

304 Thermal acceleration threshold: we quantified the acceleration of this warming  
305 and established a critical threshold of 1.04 °C·day<sup>-2</sup>. The exceedance of this threshold  
306 around nine days pre-GLOF appears to signal a critical transition in the lake-ice dam  
307 system, marking a phase of destabilization and offering a potentially robust indicator  
308 for imminent failure.

309 Cumulative thermal forcing: the strongest correlation between peak discharge and  
310 cumulative LST over 10-15 days ( $r = 0.77$ ) indicates that flood magnitude is not solely  
311 a function of an instantaneous trigger but is preconditioned by short-term, integrated  
312 thermal energy (Liu et al., 2014). The weaker correlation over 30 days suggests that the  
313 most relevant thermal forcing for outburst initiation occurs within a two-week window.

314 Integrating these signals—absolute LST, its rate of change, acceleration, and short-  
315 term cumulative temperature—can form the basis of a multi-tiered, quantitative early-  
316 warning framework that moves beyond simple lake area or level monitoring.



### 317 5.3 Generality and Limitations of the LST-GLOF Relationship

318 While this case study focuses on Lake Merzbacher, the thermal mechanisms  
319 identified are likely relevant for other ice-dammed lakes and potentially moraine-  
320 dammed lakes where thermal erosion plays a role (Debnath et al., 2018). However, the  
321 universality of our proposed thresholds (e.g.,  $12^{\circ}\text{C}$ ,  $1.04^{\circ}\text{C}\cdot\text{day}^{-2}$ ) must be tested across  
322 different geographic and geomorphic settings. It is crucial to acknowledge that GLOFs  
323 have diverse triggers. Our model best applies to gradual, thermally-driven outbursts, as  
324 opposed to those caused by dynamic, short-term triggers like ice/rock avalanches (e.g.,  
325 the 2021 Chamoli disaster), which operate on timescales of minutes to hours (Shugar  
326 et al., 2021).

327 This study has several limitations. The reliance on daily MODIS LST data may  
328 miss diurnal temperature variations critical to melt processes. We also simplified local  
329 topographic and glacier dynamic complexities (e.g., glacier surge events) to isolate the  
330 temperature signal (Häusler et al., 2016), but these factors can modulate the climatic  
331 response (Veh et al., 2025). Finally, our statistical relationships need to be grounded in  
332 physical processes through the development of coupled models that integrate surface  
333 energy balance, subglacial hydrology, and dam mechanics.

334 Future work should validate these thermal thresholds in other glacial basins using  
335 higher-resolution thermal data and incorporate detailed topographic and glaciologic  
336 data to refine predictive models and extend this early-warning methodology across  
337 High Mountain Asia.

## 338 **6. Conclusions**

339 This investigation establishes Lake Surface Temperature (LST) as a critical factor  
340 controlling the timing and magnitude of GLOFs at Lake Merzbacher. The key findings  
341 are:

342 The lake surface has warmed significantly ( $0.06^{\circ}\text{C}\cdot\text{yr}^{-1}$  for summer mean LST  
343 between 2000 and 2022), at a rate exceeding the local atmospheric warming,  
344 highlighting its role as an amplified indicator of climate change.

345 A critical LST threshold of  $12^{\circ}\text{C}$  was identified, with the vast majority of GLOFs  
346 occurring above this level, confirming the importance of thermal conditions for ice-  
347 dam stability.

348 Distinct pre-outburst thermal precursors provide actionable warning signals: a  
349 pronounced 8-day warming pulse (up to  $0.65^{\circ}\text{C}\cdot\text{day}^{-1}$ ), a critical acceleration phase  
350 ( $>1.04^{\circ}\text{C}\cdot\text{day}^{-2}$ ) around 9 days before the outburst, and a strong influence of 10–15-



351 day cumulative LST on peak discharge.

352 In conclusion, this research demonstrates that LST dynamics are a fundamental,  
353 and previously underutilized, element in understanding and predicting ice-dammed lake  
354 outbursts. The integration of real-time LST monitoring—focusing on exceedance of  
355 absolute thresholds, rates of change, and acceleration patterns—provides a robust  
356 scientific basis for enhancing early-warning systems. The methodology developed here  
357 offers a promising framework for improving GLOF risk management at Lake  
358 Merzbacher and has the potential to be adapted and applied to similar ice-dammed lakes  
359 across High Mountain Asia in a warming climate.

#### 360 **Data availability**

361 MODIS/006/MOD11A1 data for this paper are available  
362 at <https://lpdaac.usgs.gov/data>. Meteorological data are available from the China  
363 Meteorological Data Service Centre (<http://data.cma.cn/en>) upon request. The ERA5-  
364 Land dataset from the European Centre for Medium-Range Weather Forecasts  
365 (ECMWF) is available at <https://www.ecmwf.int/en/era5-land>. The basic geographic  
366 information data (River, Glacier, DEM, etc.) used in this paper are from the National  
367 Tibetan Plateau Data Centre (<https://data.tpdac.ac.cn>).

#### 368 **Acknowledgements**

369 This work was funded by the National Natural Science Foundation of China  
370 (42171148), International partnership of Chinese Academy of Science  
371 (046GJHZ2023069MI), the program of the Key Laboratory of Cryospheric Science and  
372 Frozen Soil Engineering, Chinese Academy of Sciences (No. CSFSE-ZZ-2402),  
373 Scientific Research Project of Shule River Basin Water Resources Utilization Center,  
374 Gansu Province (SLH/KYXM-2025-01), and Gansu Province Water Science  
375 Experimental Research and Technology Promotion Project (Grant No.25GSLK077).

#### 376 **Author contributions**

377 D. Shangguan initiated the idea. M. Wang, D. Shangguan and D. Li conceived the  
378 study. M. Wang and D. Li collected and processed the data. M. Wang performed the  
379 analysis, drafted the original manuscript and designed the figures. D. Shangguan, D. Li,  
380 Y. Li, R. Wang and J. Wu. A discussed the results. Q. Butt polished the manuscript. All  
381 authors reviewed and gave final approval for publication.



382 **Competing interests**

383 The authors declare no competing interests in this paper.

384 **References**

385 Aizen V B, Aizen E M, Kuzmichonok V A 2007. Glaciers and hydrological  
386 changes in the Tien Shan: simulation and prediction. *Environmental*  
387 *Research Letters*, 2: 045019.DOI:10.1088/1748-9326/2/4/045019.

388 Aizen V B, Aizen. E M 1998. Estimation of glacial runoff to the Tarim  
389 River, central Tien Shan. *IAHS Publications-Series of Proceedings*  
390 *and Reports-Intern Assoc Hydrological Sciences*, 248: 191-198.

391 Allen S K, Zhang G, Wang W, et al. 2019. Potentially dangerous glacial  
392 lakes across the Tibetan Plateau revealed using a large-scale  
393 automated assessment approach. *Science Bulletin*, 64: 435-  
394 445.DOI:10.1016/j.scib.2019.03.011.

395 Attiah G, Kheyrollah Pour H, Scott K A 2023. Lake surface temperature  
396 retrieved from Landsat satellite series (1984 to 2021) for the North  
397 Slave Region. *Earth Syst. Sci. Data*, 15: 1329-  
398 1355.DOI:10.5194/essd-15-1329-2023.

399 Austin J A, Colman S M 2007. Lake Superior summer water temperatures  
400 are increasing more rapidly than regional air temperatures: A positive  
401 ice-albedo feedback. *Geophysical Research Letters*,  
402 34.DOI:10.1029/2006GL029021.

403 Bormudoi A, Shabunin A, Hazarika M, et al. Studying the outburst of the  
404 Merzbacher lake of Inylchek Glacier, Kyrgyzstan with remote sensing  
405 and field data[C]//*Proceedings 33rd Asian Conference on Remote*  
406 *Sensing*.2012:26-30.

407 Carrivick J L, Tweed F S 2016. A global assessment of the societal impacts  
408 of glacier outburst floods. *Global and Planetary Change*, 144: 1-  
409 16.DOI:10.1016/j.gloplacha.2016.07.001.



- 410 Chen Y, Li W, Deng H, et al. 2016. Changes in Central Asia's Water Tower:  
411 Past, Present and Future. *Scientific Reports*, 6:  
412 39364.DOI:10.1038/srep39364.
- 413 Chikita K, Joshi S P, Jha J, et al. 2000. Hydrological and thermal regimes  
414 in a supra-glacial lake: Imja, Khumbu, Nepal Himalaya. *Hydrological  
415 Sciences Journal*, 45: 507-521.DOI:10.1080/02626660009492353.
- 416 Chikita K A, Yamada T 2005. The expansion of Himalayan glacial lakes  
417 due to global warming: field observations and numerical simulation  
418 [M], *Regional Hydrological Impacts of Climatic Change - Impact  
419 Assessment and Decision Making*: 111-119.
- 420 Cogley J G, Arendt A A, Bauder A, et al. 2011. Glossary of glacier mass  
421 balance and related terms [M]. IHP-VII Technical Documents in  
422 Hydrology No. 86, IACS Contribution No. 2, UNESCO-IHP; Paris,  
423 France.
- 424 Debnath M, Syiemlieh H J, Sharma M C, et al. 2018. Glacial lake dynamics  
425 and lake surface temperature assessment along the Kangchengayo-  
426 Pahunri Massif, Sikkim Himalaya, 1988–2014. *Remote Sensing  
427 Applications: Society and Environment*, 9: 26-  
428 41.DOI:10.1016/j.rsase.2017.11.002.
- 429 Glazirin G E 2010. A century of investigations on outbursts of the  
430 icedammed lake Merzbacher (central Tien Shan). *Austrian Journal of  
431 Earth Sciences*, 103: 171-179.
- 432 Gu C, Li S, Liu M, et al. 2023. Monitoring Glacier Lake Outburst Flood  
433 (GLOF) of Lake Merzbacher Using Dense Chinese High-Resolution  
434 Satellite Images. *Remote Sensing*, 15.DOI:10.3390/rs15071941.
- 435 Häusler H, Ng F, Kopečný A, et al. 2016. Remote-sensing-based analysis  
436 of the 1996 surge of Northern Inylchek Glacier, central Tien Shan,  
437 Kyrgyzstan. *Geomorphology*, 273: 292-



- 438 307.DOI:0.1016/j.geomorph.2016.08.021.
- 439 Hewitson B C, Crane R G 1996. Climate downscaling: techniques and  
440 application. *Climate Research*, 07: 85-95.DOI:10.3354/cr007085.
- 441 Hugonnet R, Mcnabb R, Berthier E, et al. 2021. Accelerated global glacier  
442 mass loss in the early twenty-first century. *Nature*, 592: 726-  
443 731.DOI:10.1038/s41586-021-03436-z.
- 444 Kingslake J, Ng F 2013. Quantifying the predictability of the timing of  
445 jökulhlaups from Merzbacher Lake, Kyrgyzstan. *Journal of*  
446 *Glaciology*, 59: 805-818.DOI:10.3189/2013JoG12J156.
- 447 Li D, Shangguan D, Huang W 2020. Research on the area change of Lake  
448 Merzbacher in the Tianshan Mountains during 1998-2017. *Journal of*  
449 *Glaciology and Geocryology*, 42: 1126-1134.
- 450 Li D, Shangguan D, Wang X, et al. 2021. Expansion and hazard risk  
451 assessment of glacial lake Jialong Co in the central Himalayas by  
452 using an unmanned surface vessel and remote sensing. *Science of The*  
453 *Total Environment*, 784:  
454 147249.DOI:10.1016/j.scitotenv.2021.147249.
- 455 Liu J 1993. Forecasting on Jokulhlaups in Kunmalike River, and its  
456 influence on river water condition, Southern Tianshan Mts.  
457 *Hydrology*: 25-30.DOI:10.19797/j.cnki.1000-0852.1993.01.006.
- 458 Liu J, Cheng Z, Su P 2014. The relationship between air temperature  
459 fluctuation and Glacial Lake Outburst Floods in Tibet, China.  
460 *Quaternary International*, 321: 78-  
461 87.DOI:org/10.1016/j.quaint.2013.11.023.
- 462 Liu J, Li Z, Liu Y. Glacier dammed lake outburst flood in cold season in  
463 the Tien Shan, China and  
464 Kyrgyzstan[C]//,2023DOI:10.20944/preprints202310.1666.v1.
- 465 Mayr E, Juen M, Mayer C, et al. 2014. Modeling Runoff from the Inylchek



- 466 glaciers and Filling of Ice-Dammed Lake Merzbacher, Central Tian  
467 Shan. *Geografiska Annaler: Series A, Physical Geography*, 96: 609-  
468 625. DOI:10.1111/geoa.12061.
- 469 Muñoz-Sabater J, Dutra E, Agustí-Panareda A, et al. 2021. ERA5-Land: a  
470 state-of-the-art global reanalysis dataset for land applications. *Earth*  
471 *Syst. Sci. Data*, 13: 4349-4383. DOI:10.5194/essd-13-4349-2021.
- 472 Ng F, Liu S 2009. Temporal dynamics of a jökulhlaup system. *Journal of*  
473 *Glaciology*, 55: 651-665. DOI:10.3189/002214309789470897.
- 474 Ng F, Liu S, Mavlyudov B, et al. 2007. Climatic control on the peak  
475 discharge of glacier outburst floods. *Geophysical Research Letters*,  
476 34. DOI:10.1029/2007gl031426.
- 477 Richardson S D, Reynolds J M 2000. An overview of glacial hazards in the  
478 Himalayas. *Quaternary International*, 65-66: 31-  
479 47. DOI:10.1016/S1040-6182(99)00035-X.
- 480 Rounce D R, Mckinney D C, Lala J M, et al. 2016. A new remote hazard  
481 and risk assessment framework for glacial lakes in the Nepal  
482 Himalaya. *Hydrol. Earth Syst. Sci.*, 20: 3455-  
483 3475. DOI:10.5194/hess-20-3455-2016.
- 484 Shangguan D, Ding Y, Liu S, et al. 2017. Quick release of internal water  
485 storage in a glacier leads to underestimation of the hazard potential of  
486 glacial lake outburst floods from Lake Merzbacher in central Tian  
487 shan Mountains: The risk of GLOF in Central Asia. *Geophysical*  
488 *Research Letters*, 44. DOI:10.1002/2017GL074443.
- 489 Shen Y, Wang G, Ding Y, et al. 2009. Changes in Merzbacher Lake of  
490 Inylchek Glacier and glacial flash floods in Aksu River Basin,  
491 Tianshan during the period of 1903-2009. *Journal of Glaciology and*  
492 *Geocryology*: 10.
- 493 Shiff S, Helman D, Lensky I M 2021. Worldwide continuous gap-filled



- 494 MODIS land surface temperature dataset. *Scientific Data*, 8:  
495 74.DOI:10.1038/s41597-021-00861-7.
- 496 Shugar D H, Jacquemart M, Shean D, et al. 2021. A massive rock and ice  
497 avalanche caused the 2021 disaster at Chamoli, Indian Himalaya.  
498 *Science*, 373: 300-306.DOI:10.1126/science.abh4455.
- 499 Thorarinsson S 1939. Chapter IX. The ice dammed lakes of Iceland with  
500 particular reference to their values as indicators of glacier oscillations.  
501 *Geografiska Annaler*, 21: 216-242
- 502 Veh G, Lützow N, Tamm J, et al. 2023. Less extreme and earlier outbursts  
503 of ice-dammed lakes since 1900. *Nature*, 614: 701-  
504 707.DOI:10.1038/s41586-022-05642-9.
- 505 Veh G, Wang B, Zirzow A, et al. 2025. Progressively smaller glacier lake  
506 outburst floods despite worldwide growth in lake area. *Nature*  
507 *Water*.DOI:10.1038/s44221-025-00388-w.
- 508 Wang X, Wu K, Jiang L, et al. 2013. Wide expansion of glacial lakes in  
509 Tianshan Mountains during 1990-2010. *Acta Geographica Sinica*, 68:  
510 983-993.
- 511 Xie Z, Shanguan D, Zhang S, et al. 2013. Index for hazard of Glacier Lake  
512 Outburst flood of Lake Merzbacher by satellite-based monitoring of  
513 lake area and ice cover. *Global and Planetary Change*, 107: 229-  
514 237.DOI:10.1016/j.gloplacha.2012.05.025.
- 515 Zhang G, Yao T, Xie H, et al. 2014. Estimating surface temperature changes  
516 of lakes in the Tibetan Plateau using MODIS LST data. *Journal of*  
517 *Geophysical Research: Atmospheres*, 119: 8552-  
518 8567.DOI:10.1002/2014JD021615.
- 519 Zheng G, Allen S K, Bao A, et al. 2021. Increasing risk of glacial lake  
520 outburst floods from future Third Pole deglaciation. *Nature Climate*  
521 *Change*, 11: 411-417.DOI:10.1038/s41558-021-01028-3.